Development of a Piezoelectric Microcompressor for a Joule-Thomson Microcryocooler

M. J. Simon[1], C. DeLuca[1], V.M. Bright[1], Y.C. Lee[1], P. E. Bradley[2], and R. Radebaugh[2]

[1]University of Colorado at Boulder, Boulder, CO
[2]National Institute of Standards and Technology, Boulder, CO 80305

ABSTRACT

In this paper we discuss the development of a microcompressor (MC) theoretically capable of delivering pressure ratios from 16:1 to 25:1 for design flow rates, of about 0.15 std. cm^3/s, intended to provide flow for a mixed refrigerant Joule-Thomson (J-T) microcryocooler. The J-T microcryocooler supports on-chip cooling applications, such as terahertz and infrared imaging sensors operating at about 77 K that require less than 5 mW of net refrigeration. The high pressure ratio of the compressor is enabled by minimizing dead volume and using a 10 mm diameter metalized polyamide membrane 500 μm thick that is actuated by a lead zirconium titanate piezoelectric (PZT) stack. With a stroke of about 28 μm and a swept volume of about 2 mm^3, the design flow rate could be achieved with a drive frequency of about 100 Hz. The entire microcryocooler, compressor module, sensor, and thermal integration module are expected to occupy less than 10 cm^3 volume. At present the compressor module demonstrates a pressure ratio of 21:1 when blanked off and has a volume less than 2 cm^3. Numerous design iterations to achieve the 21:1 ratio, studies comparing stroke and volume vs. frequency to achieve design flow rates, and measured power consumption as a function of drive frequency are discussed. Design alternatives for the valves in the compressor head, including passive micro electromechanical systems (MEMS) and active PZT, with preparations to measure pressure ratios and flow rates with both valve types also presented.

INTRODUCTION

While the development of Micro Electromechanical Systems (MEMS) technology has occurred at a relatively fast pace over the past twenty years and the ability to create incrementally more complex macroscale machines has steadily matured, the potential of conceivable devices that by necessity operate between both scale regimes remains largely untapped. The developmental account of such a scale-spanning device, a high-pressure MC, is detailed herein. The MC has been under development over the past two years as part of the larger micro-cryogenic cooler (MCC) project, a collaboration between the University of Colorado at Boulder (CU) and the National Institute of Standards and Technology (NIST), Boulder. The MCC is intended to provide cryogenic cooling via a Joule-Thomson mechanism in a small package for on-chip applications.

The intended demonstration application for the MCC is a high temperature superconducting hot-electron bolometer, which requires a temperature of approximately 77 K to operate. A concep-

Cryocoolers 15, edited by S.D. Miller and R.G. Ross, Jr.

tual view of the MCC architecture is presented in Figure 1. The MCC contains four primary subsystems, the sensor, the cold head, the heat exchanger, and the compressor.

Consistent with the Joule-Thomson effect, whereby gas temperature is decreased by expansion at constant enthalpy, when the gas temperature is below its intrinsic inversion temperature, the MCC operates as follows. Low pressure gas fills the compressor chamber through an inlet valve in the coupling. Next, the MEMS compressor is actuated to provide a high compression ratio, and the gas is expelled through an outlet valve, located within the coupling, into the heat exchanger. Moving from high pressure to low pressure, gas flows through dedicated high pressure channels in the heat exchanger, where it reaches the cold head, it expands fully and cools the cold head. Expanded low pressure gas returns to the coupling through the dedicated low pressure channels within the heat exchanger and the cooling cycle continues.

To function harmoniously as part of the larger MCC system, the MC had to meet specific requirements. A generated compression ratio of between 16:1 and 25:1 and a fluid flow rate of approximately 0.15 std. cm^3/s had to be achieved, a mean power close to 200 mW, and a volume of about 1 cm^3 were desired.

PRIOR ART

Micro Pumps

Most previously developed micro pumps and compressors were intended for low pressure micro-fluidic applications. Reviewed pumps operated using a uni- and a bimorph piezoelectric disk actuation. Linnemann[1] described a silicon piezoelectric bimorph square membrane diaphragm pump with 5.7x5.7 mm^2 active area and an achieved 1:9 compression ratio. Driven using -40 V to +120 V, the disk actuator provided 14 µm displacement. Operated at 220 Hz, the device could sustain a flow rate of approximately 1 mL/min. Similarly Saggere[2] used a bonded piezoelectric cylinder and silicon circular membrane with ~10.2 mm^2 active area to achieve a flow rate of 2.5 mL/min using 1200 V actuation voltage and a 4.5 kHz drive frequency. Hayamizu[3] presented an analogous configuration with comparable performance. The packaged device has dimensions of 20x35x0.7 mm^3. The research in Feng[4] offered similar dimensions of 13x13x1.2 mm^3 with 0.04 atm. pressure generation. Yang[5] demonstrated that a 100 µm thick piezoelectric stainless steel bimorph diaphragm, operating at 120 Hz resonance frequency, was capable of providing a 4.5 mL/s flow rate. It featured a membrane displacement of 410 µm with a 20 V drive voltage, and had a maximum power draw of 3.18 mW. Packaged dimensions were 60x16x2 mm^3. Most recently Wu[6] presented a bimorph piezoelectric pump with actuation voltage of 100 V peak-to-peak featured a 0.05 std. cm^3/s flow rate and 0.04 atm. pressure generation. The packaged device size was 13x13x1.2 mm^3 and used ~10 W power. Delving into the micro turbine for power generation realm, one exposes more designs akin to macroscale compressors. Peirs[7] showed that a micro gas turbine with a rotor diameter of 10 mm was capable of generating a pressure ratio of 1.20.

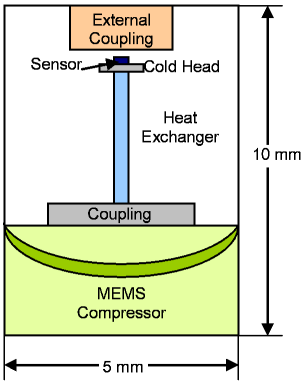

Figure 1. MCC subsystem schematic.

MEMS Valves

Three categories of passive MEMS valves have been explored by other authors. The first are bivalvular systems made entirely out of single silicon wafers (see Smith[8] and Yang[9]) that can be fabricated using a minimum number of process steps. Second are flapper valves fabricated using silicon wafers with deposited layers of polysilicon (Bien[10]), parlyene (Feng[4]), and nickel (Li[11]). The third, dynamic valve systems, have also been made entirely out of silicon as in Gerlach[12-14], and offer greatly simplified geometry.

Unfortunately, the simplicity of the bivalvular designs limits their performance. Specifically in compressor applications, the triangular geometry creates dead volume, which adds to the swept volume and therefore lowers the achievable compression ratio. In Smith[8] and Yang[9] the maximum back pressure was never postulated. However, Yang[9] applied back pressures up to 4 kPa (about 0.04 atm.) to ascertain back flow characteristics. The reverse flow at this pressure was found to be low (~0.05 std. cm^3/min). Forward flow rates of ~0.33 std. cm^3/s were achieved. Smith[8] and Yang[9] created valve flexures using diffusion boron doping followed by back side etching. This process limited the achievable thickness of the valve flexures.

Some flapper valve systems have very desirable performance characteristics but their fabrication can in-practice be fairly difficult, requiring numerous fabrication steps and two bonded silicon wafers (see Li[11]). Typically, flapper valves are fabricated with cantilever type or bridge type flappers. In both Feng[4] and Li[11], opposing flappers were fabricated on two different silicon wafers. Then the wafers were bonded together to construct a complete valve system: one valve for inflow and another for outflow. Li[11] demonstrated an approximately 18 std. cm^3/s flow rate and postulated that ~90 atm. back pressures were possible. In Bien[10] a design was presented that would allow for fabrication of opposing valves on a single chip, albeit using a fabrication process more complicated than that used to construct bivalvular systems. Flow rates up to ~0.07 std. cm^3/s and back pressures up to 0.1 atm. were achieved.

Dynamic valve systems operate quite differently than the other types. The most unique feature of dynamic valve systems is the lack of any seal mechanism. Dynamic valves mandate that the fluid flows turbulently into and out of the pump chamber to create a directional flow (Gerlach[12]). Turbulent flow in the positive direction causes a free jet to flow out of the dynamic valve. Turbulent flow through the negative direction causes a separation in the boundary layer which causes flow in the negative direction to require more energy than in the positive direction. This positive vs. negative flow difference causes a net flow in the positive direction if the pumping membrane is oscillated at sufficiently high frequencies: on the order of kilohertz (Gerlach[12-14]). Dynamic valve fabrication processes employ a single Potassium Hydroxide (KOH) etch step. Optimized micropumps with dynamic valve systems have been shown to be capable of producing fairly high flow rates (~0.122 std. cm^3/s (Gerlach[14]), but the generated pressure is quite small (~0.07 atm. Gerlach[12]).

DESIGN AND ANALYSIS

Systems Engineering

A process of systems engineering was employed to tackle the functional requirements decomposition deemed necessary to accomplish the scale bridging. In this manner, an optimal design was quickly achieved by providing a method to eliminate inferior design alternatives. Trade matrix and trade flows were both developed to identify the important system design parameters and how their interrelationships affected predicted system performance. This combination of systems engineering techniques showed how meeting requirements and derived requirements necessitated compromises between the importance of each parameter and the parameter choices. To implement a high force, small size, and low power actuation solution, it was quickly discerned that piezoelectric actuation was the method of choice. A custom all piezoelectric membrane was initially considered, but analyses quickly showed that the membrane thickness necessary to generate the required displacement was too thin (~2 μm) to withstand a working pressure of 25 atm. Thus a decision to use a PZT stack design was made.

Actuator and Membrane Sizing

Rather than undertake customized PZT stack development, it was decided to expedite a proof-of-principle piezoelectric compressor demonstration. Therefore, a survey of commercial-off-the-shelf (COTS) PZT actuators was conducted and a representative straw man actuator was chosen as possessing length and width dimensions between 3 mm and 5 mm and a displacement of 10 -30 µm. Most critical to this application is the force generated by the actuator. Obviously at a minimum, the resulting force on or generated by the membrane actuator assembly should be equivalent to the maximum desired force of 25 atm. (40.5301 N for a 4x4 mm^2 membrane) for a given membrane area. As the surveyed COTS actuators have blocking forces in the range of hundreds of Newton, they are deemed sufficient for this purpose.

The required force can be calculated using Eq. (1), where P is the pressure in Pa, A is the area in m^2, and F is the force in N.

$$P = \frac{F}{A} \tag{1}$$

Whether circular or square, the appropriate membrane thickness can be derived approximately by considering the realized actuator force and the chosen membrane material's Young's Modulus in conjunction with the static plate equation for a circular membrane. Eq. (2), where $\ddot{a}_{MAX}=\ddot{A}_{thk}$ *(m)* is the displacement, E is Young's Modulus (N/m^2), v is Poisson's Ratio, and *thk* is the membrane thickness (m) is defined as:

$$thk = \sqrt[3]{\frac{3\,\mathrm{Pr}^4\left(1-v^2\right)}{16E\delta_{MAX}}} \tag{2}$$

An optimization analysis was conducted with MATLAB using a number of membrane material properties. Results show that for stainless steel and silicon, assuming 10 µm displacement, a membrane approximately 400 µm thick would suffice while a polyamide membrane would need to be over 1 mm thick.

Swept Volume

A finite element model (FEM) of the membrane was constructed using CoventorWare. A force of 40.5301 N was applied to the bottom of a 400 µm thick membrane perpendicular to a 3.5x3.5 mm face (representing the actuator surface) adjoining the actuator and the membrane. Deformed mesh results (height scaled by a factor of 100) can be seen below in Figure 2a. The mesh interior provided a numerically computed swept volume. Both stainless steel and silicon membrane materials were simulated with similar thickness results. To ascertain the approximate swept volume, the FEM mesh data was exported into MATLAB where a convex hull algorithm was used on the mesh interior nodal positions. The numerically computed swept volume was 1.1506×10^8 μm^3. The extracted swept volume can be seen below in Figure 2b.

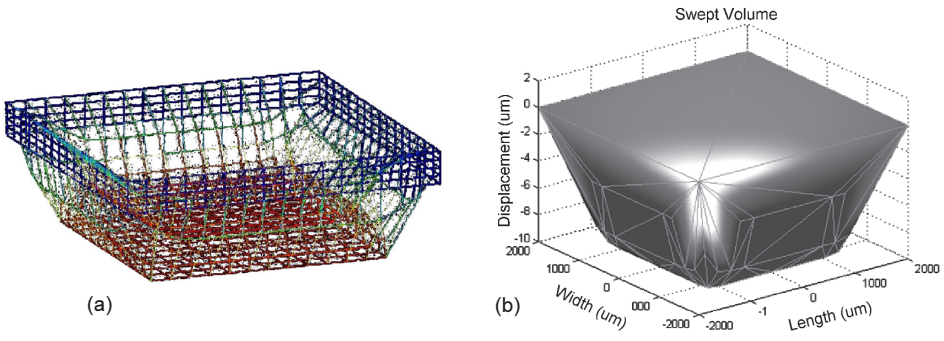

Figure 2. (a) Deformed FEM membrane mesh scaled by a factor of 100 to enhance visualization and (b) the swept volume computed using a convex hull method enabled actuator sizing.

Drive Frequency Scaling

The volume flow rate requirement Vol_{FLOW} was 0.112 cc/s, equivalent to 1.126656×10^{11} μm³/s. Flow rate divided by the swept volume Vol_{SWEPT}, as in Eq. (3), yielded the necessary drive frequency f_D of approximately 1 kHz.

$$f_D = \frac{Vol_{FLOW}}{Vol_{SWEPT}} \tag{3}$$

In general piezoelectric actuators heat internally with increasing drive frequency. Typically, drive frequencies do not exceed 300 Hz. Therefore, a subsequent analysis was conducted to determine the drive frequency sensitivity as a function of membrane displacement with a membrane length and a width dimensions of both 3.5 mm and 4 mm. As can be seen in Figure 3, the required drive frequency decreases exponentially with monotonically increasing displacement. This indicated that increasing the actuator displacement to values above approximately 25 μm would allow typical actuator drive frequencies to be employed. This knowledge enabled selection of an appropriate COTS PZT stack actuator.

Compressor General Design

The general compressor design included elements that were intended to afford proof-of-principal demonstration and ease of assembled device testing. Consequently, the compressor structure was divided into several modular substructures and combined into one primary assembly shown below in Figure 4. Designated substructures included a base plate, an actuator structure, and a sensor housing cap. It was envisioned that all three components would be connected together using machine screws (tap holes and screws not depicted) to accommodate ease of assembly and disassembly. The actuator would fit with a little gap within the actuator structure. The actuator would be bonded to both the actuator structure at the membrane and the actuator chuck. For setup testing, the actuator membrane complex would be given an initial displacement less than the maximum possible actuator displacement using the micrometer set screw. The micrometer set screw would then be attached to the bottom of the actuator chuck through the base plate. An initial membrane displacement would be desired, so that the actuator acted preferentially for maximal extension during the upward stroke and the membrane would be prestressed. A check valve would be press-fit between the sensor housing cap and the actuator structure. The inlet and outlet, the sensor housing cap, the check valve, and the actuator structure would be sealed. The sensor housing cap would incorporate the dedicated inlet and outlet channels. The outlet would include cutouts for total and static pressure transducers. The pressure transducers would also be sealed to the sensor housing cap. All structural components would be machined from stainless steel.

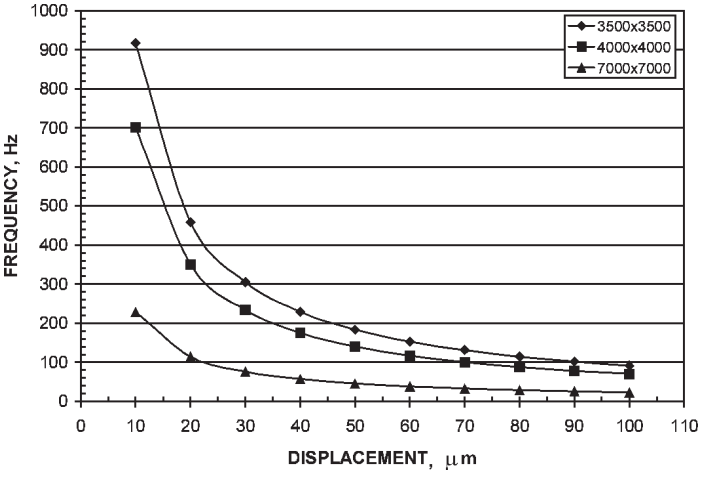

Figure 3. Plotting drive frequency as a function of membrane displacement afforded component sizing that met requirements. Legend units are micrometers.

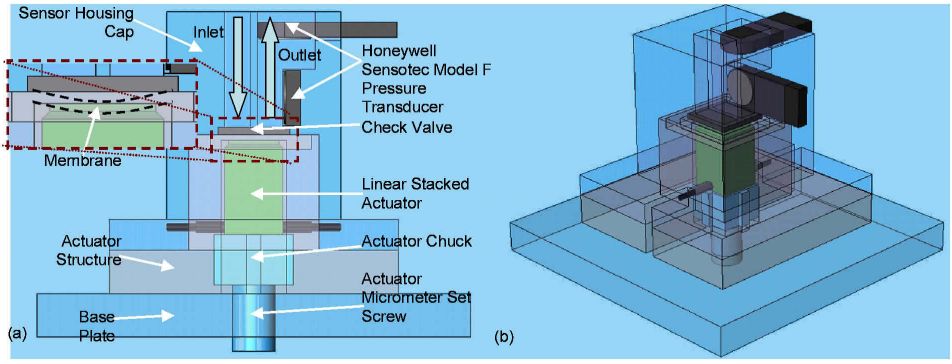

Figure 4. General compressor assembly schematic (a) side view and (b) perspective view.

Check Valve General Design

To accommodate the operational simplicity, it is desirable to have a check valve with a passive design. The valve sizing analysis results and references cited above, suggested a general design where the valve geometry would serve to allow inlet flow while impeding outlet flow. On the membrane down stroke, the inlet openings would be open as a function of the pressure exerted by the downward flow and the outlet openings would be closed. Figure 5b shows this action in the schematic section view. At the inlet, the downward pressure would act on the inward, down angled opening surfaces, and force the valve open. Conversely, at the outlet, the downward pressure would act on the inward, up angled opening surfaces, and force the valve closed. Upon the up stroke, the valve being functionally symmetric, would act in reverse. It is important to note that the deforming portion of the valve structure can be tailored such that the portion thickness is sufficient to achieve appropriate cracking pressure. The check valve would be made from etched silicon.

PROTOTYPE FABRICATI ON, INTEGRATION, AND TEST

Compressor

Beginning with the general design as described above, the compressor went through three generations of development until the desired pressure range was achieved. For reasons of fabrication simplicity, a design that favored a circular membrane over a square membrane was chosen, although the actuators of choice were rectangular. The actuators used for all prototypes were manufactured by APC International, Ltd.; models Pst 150/3.5x3.5/7 and Pst 150/3.5x3.5/20 were used and had dimensions and displacements of 9x3.5x3.5 mm, 18x3.5x3.5 mm, 10 µm, and 30 µm respectively. Each required -30 V to +150 V for full stroke. An APC International, Ltd. SVR-500 model amplifier with a range of -100 V to +500 V was selected to amplify the sinusoidal drive signal from a standard -1 V to +1 V waveform generator.

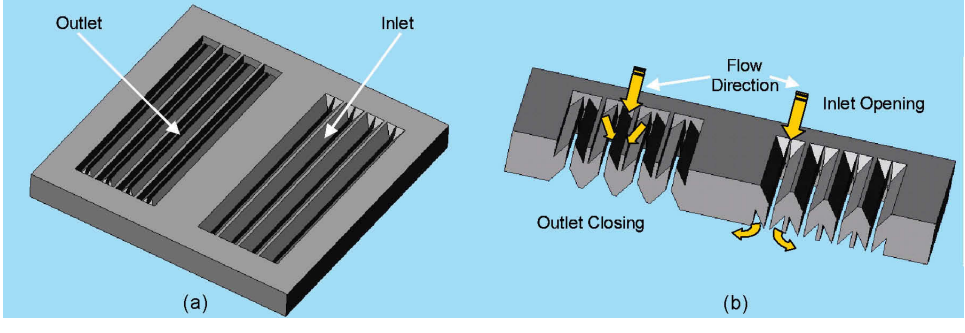

Figure 5. (a) Passive valve schematic and (b) section.

The winning design possessed several key features: all critical to eliminating device failure (see Figure 6). First, a membrane separate from the actuator structure that was clamped in place and sealed when the sensor cap was in-place proved to be essential. Second, maximizing bonding surface area between the actuator and the membrane prevented membrane delamination. This evolved into a design where the actuator was first epoxied to a brass piston head which was in turn bonded to the membrane, the method of bonding dependent on the membrane; metalized Kapton™ membranes were soldered, while latex membranes were epoxied. Third, a micrometer set screw with a hexagonal head for initial membrane pull-down insured proper mechanical advantage and position control.

Initial pressure tests were designed to determine the maximum pressure wave that could be generated using this class of device. Honeywell Sensotec Model S Pressure Transducers with a calibrated maximum pressure of 500 psi were incorporated into a sensor housing cap to facilitate measurement. A latex rubber seal was also used inside the sensor cap.

Two membrane materials were tested: copper metalized Kapton™ 500 µm thick and latex rubber 635 µm thick. The latex rubber membranes being epoxied to the piston head saw rapid degradation of adhesion during testing, while the Kapton™ membranes solder bonded to the brass piston head showed no signs of bond degradation after many operational cycles. Drive frequencies of 0.5-50 Hz were run for both latex and stainless steel membranes. A 10 Hz drive frequency using a steel membrane yielded a 21.654 atm. relative gauge pressure difference. The minimum pressure was -10.625 psig and the maximum pressure was 307.6 psig. For drive frequencies greater than 50 Hz, the SVR-500 model amplifier failed to provide the required voltage range for full stroke, which resulted in significant pressure drop.

Measured Compressor Power Consumption

To achieve maximum pressure for drive frequencies greater than 50 Hz, and adequately measure power consumption, a single channel Trek, Inc. model PZD350-1-L-CE, high-voltage amplifier was used. This amplifier was capable of achieving the required voltage range in excess of 300 Hz drive frequencies. Drive frequencies ranging from 10 to over 200 Hz were tested. Results beyond 200 Hz were not measured as the LabView DAQ used was limited to +/- 100 mA current acquisition, which caused signal clipping around 200 Hz and subsequently unreliable power readings. The generated pressure waves as functions of time for all drive frequencies were analogous to those shown in Figure 7. Figure 8 depicts the average power a function of drive frequency, and importantly that a drive frequency of approximately 60 Hz meets the 200 mW power requirement.

Passive Valve

A series of custom MATLAB scripts were created to parameterize the most important valve features and generate valve geometry for subsequent mask generation. This was done to facilitate rapid rework of the entire valve design process. Parameters included but were not limited to: valve length and width, valve opening width and depth, and wafer material dependent etch angle (54.74° for [100] silicon).−Several rounds of valve fabrication have been conducted to optimize resultant feature geometry and are ongoing (Figure 9). In all cases valves were fabricated on a 76.2 mm

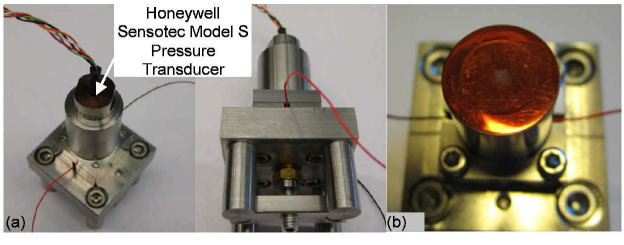

Figure 6. Third generation prototype (a) and (b) depression in the metalized Kapton™ diaphragm was created by the generated pressure during operation

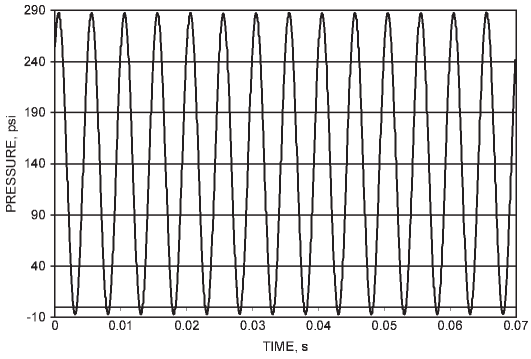

Figure 7. Generated pressure wave of 20 atm. at 200 Hz drive frequency as a function of time.

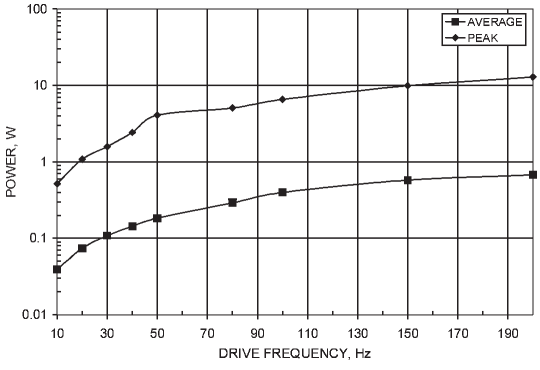

Figure 8. Actuator average and peak power draw as a function of drive frequencies from 10 to 200 Hz.

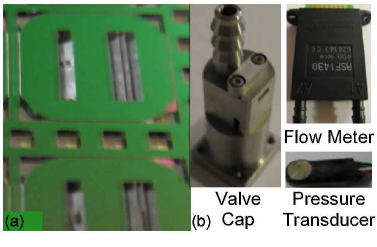

Figure 9. Example of a micromachined passive valve (a) and (b) valve pressure and flow rate transducers.

diameter 500 µm thick silicon wafer [100] crystal orientation (double-side polished) with 3 µm oxide layer on both faces. Four inch glass masks were used for lithography with a positive photoresist. Wafers were then etched front and back side using KOH solution. A sensor housing cap to interchangeably hold a variety of passive valves was designed and fabricated. The cap incorporated two Honeywell Sensotec Model F Subminature Low Profile Pressure Transducers in the outlet channel, one to measure the static pressure and the other to measure the total pressure; from which the dynamic pressure could be computed. They could sense a calibrated maximum pressure of 500 psi. To measure flow rate, it is planned that the inlet channel e connected to a Sensiron ASF1430 Digital Gas Flow sensor which in turn will feed into LabView through the ITL DAQ.

Active Valve

As a risk mitigation measure, an active valve was also considered. Two active valves were designed and fabricated each accommodating two different PZT actuators, one thinner (the APC

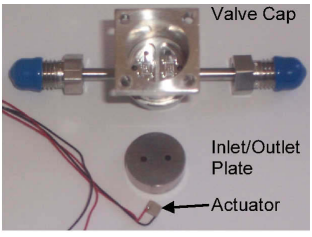

Figure 10. Active valve components prior to assembly.

International, Ltd. Pst150/3x3/2) with 3 µm stroke capability, and one thicker (Pst150/2x3/7) with 15 µm stroke capability. Each required -30 V to +150 V for full stroke. The active valve assembly took the place of the sensor housing cap in previous prototypes. VCR connectors were also employed for ease of integration with the cryocooler prototype. The valve control signals were provided by LabView through a National Instruments USB-6259 M Series DAQ to a dual channel version of the Trek high-voltage amplifier, one channel per actuator. As of publication the active valves have been assembled, but are yet to be tested (Figure 10).

CONCLUSIONS AND FUTURE WORK

A novel micro/macro scale spanning micro compressor capable of generating high pressures was successfully developed and demonstrated. Systems engineering principles were judiciously applied to analyze the design trade space and map functional requirements to available technologies. The resulting series of iteratively refined prototypes yielded measured blanked off pressures and power consumptions within close range of design targets. In addition, the initial development of two distinct valve configurations, passive and active, was presented with plans for subsequent integration and testing. Future work will focus on compressor pressure-volume curve generation, actuator heating measurement as a function of drive frequency, compressor integration with the MCC and demonstration of closed-loop cooling, and multistage designs for greater pressure ratios.

ACKNOWLEDGMENT

The authors generously thank Eyal Gerecht and James Booth from NIST, Boulder for their many contributions and kind assistance. We also would like to extend warm appreciation to Charlie Bowen and Tracy Buxkemper from the CU Duane Physics machine shop and Jim Kastengren from the CU CIRES instrument shop for their outstanding design suggestions and superior craftsmanship. Funding from the Defense Advanced Research Projects Agency (DARPA) Microcryocooler (MCC) program is acknowledged.

REFERENCES

1. Linnemann, R., et al., “A Self-Priming and Bubble-Tolerant Piezoelectric Silicon Micropump For Liquids and Gases,” *MEMS 1998*, 25-29 Jan 1998, pp. 532 – 537.
2. Saggere, L., et al., “Design, Fabrication, and Testing of a Piezoelectrically Driven High Flow Rate Micro-Pump,” *ISAF 2000*, pp. 297 - 300.
3. Hayamizu, S. et al., “New Bi-Directional Valve-Less Silicon Micro Pump Controlled By Driving Waveform,” *MEMS 2002*, pp. 113 – 116.
4. Feng, G. et al., “Micropump Based on PZT Unimorph and One-Way Parylene Valves,” *Journal of Micromechanics and Microengineering,* Vol. 14, No. 4 (April 2004), pp. 429 – 435.
5. Yang, X., et al., “Simulation and Experimental Studies on a Piezoelectrically actuated Microdiaphragm Air Pump,” *J. Microlith., Microfab., Microsyst.* 5(2), 021106 (Apr-Jun 2006).
6. Wu, C. et al., “Low Power Consumption PZT Actuated Micro-Pump,” *IMPACT 2006*, 18-20 Oct. 2006, pp. 1-4.

7. Peirs, J. et al., "A Micro Gas Turbine Unit for Electric Power Generation: Design and Testing of Turbine and Compressor," *Actuator 2004*, 14-16 June 2004, pp. 796 - 799.

8. Smith, L. et al., "A Silicon Self-Aligned Non-Reverse Valve," *Transducers '91*, June 24 – 27, 1991, pp. 1049 - 1051.

9. Yang, E.H. et al., "Fabrication and Testing of Passive Biavulvar Microvalves Composed of p+ Silicon Diaphragms," *Sensors and Actuators*, Vol. 57, No. 1, pp. 75 – 78 (Oct. 1996).

10. Bien, D.C.S., et al., "Fabrication and Characterization of a Micromachined Passive Valve," *Journal of Micromechanics and Microengineering*, Vol. 13, No. 5, (Apr. 2003) pp. 557 – 562.

11. Li, B. et al., "Development of Large Flow Rate, Robust, Passive Micro Check Valves for Compact Piezoelectrically Actuated Pumps," *Sensors and Actuators*, Vol. 117, No. 2, (Jan. 2004) pp. 325- 330.

12. Gerlach, T. et al., "Working Principle and Performance of the Dynamic Micropump," *MEMS 1995*, Jan. 29 – Feb. 2, 1995, pp. 221 - 226.

13. Gerlach, T. et al., "A New Micropump Principle of the Reciprocating Type Using Pyramidic Micro Flowchannels as Passive Valves," *Journal of Micromechanics and Microengineering*, Vol. 5, No. 2, pp. 199 – 201 (June 1995).

14. Gerlach, T., "Pumping Gases by a Silicon Micro Pump with Dynamic Passive Valves," *Transducers '97*, June 16-19, 1997, pp. 357 – 360.